Mon. Not. R. Astron. Soc. **000**, 000–000 (0000) Printed 5 February 2008 (MN LATEX style file v2.2)

On the relation between electron temperatures in the O^+ and O^{++} zones in high-metallicity H II regions

Leonid S. Pilyugin[1], José M. Vílchez[2] and Trinh X.Thuan[3]
[1] *Main Astronomical Observatory of National Academy of Sciences of Ukraine, 27 Zabolotnogo str., 03680 Kiev, Ukraine (pilyugin@mao.kiev.ua)*
[2] *Instituto de Astrofísica de Andalucía, CSIC, Apdo, 3004, 18080 Granada, Spain (jvm@iaa.es)*
[3] *Astronomy Department, University of Virginia, P.O.Box 3818, University Station, Charlottesville, VA 22903 (txt@virginia.edu)*

Accepted 2006 May 25. Received 2006 May 25; in original form 2006 April 13

ABSTRACT
We suggest a new way to establish the relation between the electron temperature t_3 within the [O III] zone and the electron temperature t_2 within the [O II] zone in high-metallicity (12+log(O/H) > 8.25) H II regions. The t_2 – t_3 diagram is constructed by applying our method to a sample of 372 H II regions. We find that the correlation between t_2 and t_3 is tight and can be approximated by a linear expression. The new t_2 – t_3 relation can be used to determine t_2 and accurate abundances in high-metallicity H II regions with a measured t_3. It can also be used in conjunction with the ff relation for the determination of t_3 and t_2 and oxygen abundances in high-metallicity H II regions where the [OIII]λ4363 auroral line is not detected. The derived t_2 – t_3 relation is independent of photoionization models of H II regions.

Key words: galaxies: abundances – ISM: abundances – H II regions

1 INTRODUCTION

Accurate abundances in H II regions can be derived via the classic T_e method, T_e being the electron temperature of the H II region. In this method, the reliability of the equations for determining the O^{++}/H^+ and O^+/H^+ ionic oxygen abundances depends to a great part on the reliability of the atomic data. Pilyugin & Thuan (2005) have compared the ionic oxygen abundances derived with a recent set of equations using the latest atomic data (Izotov et al. (2006)), with those determined from an earlier set of equations (Pagel et al. (1992)) and have found close agreement. Thus, the equations for the determination of the ionic oxygen abundances in H II regions appear to be robust, in the sense that, for a given set of measured electron temperatures t_3 and t_2, relations determined by different authors result in close oxygen abundances in H II regions.

The electron temperatures t_3 within the [O III] zone and t_2 within the [O II] zone are determined from diagnostic line ratios when they are available. The intensity ratio of the [O III]λ4959 + λ5007 nebular line to the [O III]λ4363 auroral line is used to determine t_3. As for t_2, the intensity ratio of the [O II]λ3727 nebular line to the [O II]λ7320+λ7330 auroral line is used. Based on a sample of H II regions where all the necessary oxygen lines are detected, Kennicutt et al. (2003) found that the t_2 temperatures show a large scatter and that they are nearly uncorrelated with t_3 temperatures. They noted that the measurements of the faint [O II]λ7320+λ7330 auroral lines may contain large random errors. Furthermore, Rubin (1986); Tsamis et al. (2003) have pointed out that the [O II]λ3727/[O II]λ7320 + λ7330 ratio may be affected by recombination. Izotov et al. (2006) have derived t_2 and t_3 from the above ratios for a sample of H II regions. They concluded that the two temperatures generally follow the t_2 – t_3 relation obtained from photoionization models (e.g. Stasinska 1982, 1990), but that the scatter of the data points is very large. The large scatter was attributed to large flux errors of the weak [O II]λ7320 + λ7330 emission lines.

The intensity ratio of the [N II]λ6548 + λ6584 nebular line to the [N II]λ5755 auroral line is also used to determine t_2. It seems to give more reliable values. However, the contribution of recombination to the excitation of the [N II]λ5755 line may affect temperatures derived from the [N II] nebular to auroral line ratios (Rubin 1986; Tsamis et al. 2003). The ([N II]λ6548 + λ6584)/[N II]λ5755 ratio is measured in only a few H II regions with a detected ([O III]λ4959 + λ5007)/[O III]λ4363 line ratio.

When only a single temperature measurement is available, a t_2 – t_3 relation based on grids of H II region models is usually used. Several versions of such a t_2 – t_3 relation have been proposed (e.g. Campbell et al. 1986; Pagel et al. 1992; Izotov et al. 1997; Deharveng et al. 2000; Oey & Shields 2000), but the agreement between them is not very good. The available measurements do not provide an undisputable evidences in favour of any out of suggested relations, i.e. the choice of the relation is in fact arbitrary.

Thus, the t_2 – t_3 relation seems to be the weakest link of the classic T_e method. We will address this problem here.

The main goal of this paper is to derive a t_2 – t_3 relation which is model-independent. This allows one to relax the arbitrarity in the choice of the t_2 – t_3 relation. The basic idea is the following. Usually, the set of equations used for the determination of the ionic O^{++}/H^+ and O^+/H^+ abundances in H II regions is applied to the whole nebula. If we apply the equation for O^{++}/H^+ only to the O^{++} zone, then this would yield, not the ionic O^{++}/H^+ abundance, but the total O/H oxygen abundance instead. There is no reason to suspect that the oxygen abundances in the O^{++} and O^+ zones differ. We therefore require that the equation for O^{++}/H^+ applied to the O^{++} zone and the one for O^+/H^+ applied to the O^+ zone result in exactly the same value of the oxygen abundance. This condition allows us to derive a relation between t_2 and t_3. We can apply the equation for O^{++}/H^+ to the O^{++} zone alone, only if we know the contribution of the O^{++} zone to the measured H_β flux of the H II region. We will be using the ff relation (Pilyugin 2005; Pilyugin et al. 2006) for this purpose.

The observational sample to be used is described in Section 2. The strategy for determining the t_2 – t_3 relation is discussed in Section 3. A model-independent t_2 – t_3 relation is derived in Section 4. We discuss the results in Section 5, and summarize our conclusions in Section 6.

We will be using the following notations throughout the paper: $R_2 = I_{[OII]\lambda3727+\lambda3729}/I_{H_\beta}$, $R_3 = I_{[OIII]\lambda4959+\lambda5007}/I_{H_\beta}$, $R = I_{[OIII]\lambda4363}/I_{H_\beta}$, $R_{23} = R_2 + R_3$. With these definitions, the excitation parameter P can be expressed as: $P = R_3/(R_2+R_3)$.

2 OBSERVATIONAL DATA

A large sample of high-precision measurements of H II regions is at the base of the present investigation. We include first the sample of Pilyugin & Thuan (2005) who have carried out an extensive search of the literature to compile a list of more than 700 individual spectra of H II regions in irregular and spiral galaxies, with the requirement that they all possess a detected [O III] λ4363 emission line. While we have tried to include as many sources as possible, we do not claim our search to be exhaustive. Since the majority of extragalactic H II regions are in the low-density regime (Zaritsky et al. 1994; Bresolin et al. 2005), only such H II regions will be considered here. Of the objects with the electron density-sensitive ratio r_n = [S II] λ6716/[S II] λ6731 available, those with $r_n < 1.3$ were excluded.

We have also included the sample of Izotov et al. (2004, 2006) who have extracted from the Data Release 3 of the Sloan Digital Sky Survey (SDSS) around 4500 spectra of H II regions with an [O III] λ4363 emission line detected at a level better than 1σ, and carefully measured the line intensities in each spectrum. The SDSS H II regions are also in a low-density regime. Yuri Izotov and Natalia Guseva have kindly provided us with the total list of their measurements, as only part of these have been published (Izotov et al. 2004, 2006). In total, our sample consists of around 5200 H II region spectra.

Following Pilyugin & Thuan (2005), we can use the the ff relation (Pilyugin et al. 2006) to select out the H II regions with the highest quality measurements. We can define a "discrepancy index", equal to the difference between the logarithm of the observed flux R^{obs} in the [O III]λ4363 line and the logarithm of the flux R^{cal} of that line derived from the strong [O II]λ3727, [O III]$\lambda\lambda$4959,5007 lines using the ff relation:

$$D_{ff} = \log R^{obs} - \log R^{cal}. \quad (1)$$

It is well known that the relation between the oxygen abundance and the strong oxygen line intensities is double-valued, with two distincts parts, traditionally known as the upper high-metallicity branch and the lower low-metallicity branch of the R_{23} – O/H diagram. Following Pilyugin & Thuan (2005), we adopt the value of 12+log(O/H) = 8.25 as the boundary between the upper branch and the transition zone. The exact boundary is difficult to establish, but we have chosen that value because we will be using later the ff relation which is applicable at metallicities above 12+log(O/H) $\sim$ 8.25. We have extracted from our total sample a subsample of high-metallicity H II regions with an oxygen abundance 12+log(O/H) > 8.25. The oxygen abundances have been calculated with the equations of Izotov et al. (2006) for the T_e method, and with the t_2 – t_3 relation of Campbell et al. (1986). Fig. 1 shows the cumulative number of individual H II region measurements with the absolute value of the discrepancy index D_{ff} less than a certain value. Solid and open circles show data for H II regions with respectively positive and negative values of the discrepancy index. It is seen that the agreement between the cumulative numbers of measurements with positive and negative values of the discrepancy index D_{ff} is good for values of D_{ff} less than 0.05, but gets increasingly worse at higher values. This is the result of a selection effect. Indeed, a large positive value of D_{ff} means that the observed R^{obs} is significantly overestimated. This leads to a substantial overestimate of the electron temperature and an underestimate of the oxygen abundance, bringing it lower than our metallicity cut-off of 12+log(O/H) = 8.25. This effect thus systematically depletes the number of high-metallicity H II regions with a large positive D_{ff}. To free ourselves from this systematic effect, we select only measurements with the absolute value of D_{ff} less than 0.05. This sample contains 372 data points and will be referred to as the standard sample. The H II regions in it have line intensity errors that are random.

3 A STRATEGY FOR THE DETERMINATION OF THE t_2 – t_3 RELATION

3.1 The usual version of the T_e method

For abundance determination in an H II region, a two-zone model for its temperature structure is usually adopted. Izotov et al. (2006) have recently published a set of equations for the determination of the oxygen abundance in H II regions in the context of such a two-zone model. According to those authors, the electron temperature t_3 within the [O III] zone, in units of 10^4K, is given by the following equation

$$t_3 = \frac{1.432}{\log(R_3/R) - \log C_T}, \quad (2)$$

The quantity C_T is defined by:

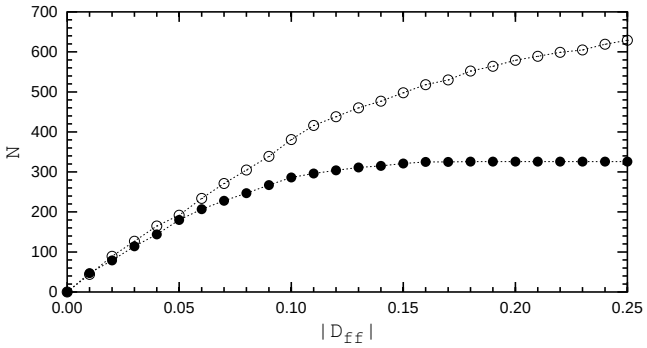

Figure 1. Cumulative number of individual measurements of H II regions with the absolute value of the discrepancy index D_{ff} less than a given value. The solid circles show data for H II regions with positive values of the discrepancy index, and the open circles for H II regions with negative values of the discrepancy index.

$$C_T = (8.44 - 1.09\,t_3 + 0.5\,t_3^2 - 0.08\,t_3^3)\,v, \quad (3)$$

where

$$v = \frac{1 + 0.0004\,x_3}{1 + 0.044\,x_3}, \quad (4)$$

and

$$x_3 = 10^{-4} n_e t_3^{-1/2}. \quad (5)$$

As for the ionic oxygen abundances, they are given by the following equations:

$$12 + \log(O^{++}/H^+) = \log(I_{[OIII]\lambda4959+\lambda5007}/I_{H_\beta}) + 6.200 + \frac{1.251}{t_3} - 0.55\log t_3 - 0.014\,t_3, \quad (6)$$

and

$$12 + \log(O^+/H^+) = \log(I_{[OII]\lambda3727+\lambda3729}/I_{H_\beta}) + 5.961 + \frac{1.676}{t_2} - 0.40\log t_2 - 0.034\,t_2 + \log(1 + 1.35x_2), \quad (7)$$

where

$$x_2 = 10^{-4} n_e t_2^{-1/2}. \quad (8)$$

Here n_e is the electron density in cm^{-3}.

The total oxygen abundances are then derived from the following equation:

$$\frac{O}{H} = \frac{O^+}{H^+} + \frac{O^{++}}{H^+}. \quad (9)$$

The electron temperature t_2 of the [O II] zone is usually determined from an equation which relates t_2 to t_3, derived by fitting H II region models. Several versions of this t_2 – t_3 relation have been proposed. A widely used relation is the one by Campbell et al. (1986) (see also Garnett (1992)) based on the H II region models of Stasińska (1982):

$$t_2 = 0.7\,t_3 + 0.3. \quad (10)$$

Another relation has been proposed by Pagel et al. (1992), also based on H II region models of Stasińska (1990))

$$\frac{1}{t_2} = 0.5(\frac{1}{t_3} + 0.8). \quad (11)$$

Izotov et al. (1997), fitting also the H II region models of Stasińska (1990), have proposed the following expression

$$t_2 = 0.243 + 1.031\,t_3 - 0.184\,t_3^2. \quad (12)$$

Based on H II region model calculations by Stasińska & Schaerer (1997), Deharveng et al. (2000) have suggested the following relation

$$t_2 = 0.775\,t_3 + 0.281. \quad (13)$$

Oey & Shields (2000) have found that the Campbell et al. relation is reasonable for $t_3 > 1.0$. However at lower temperatures, the models are more consistent with an isothermal nebula. They consequently adopted the formulation,

$$t_2 = \begin{cases} 0.7\,t_3 + 0.3, & t_3 > 1.0 \\ t_3, & t_3 < 1.0. \end{cases} \quad (14)$$

Using the system of equations Eqs.(2)÷(9) and one of the t_2 – t_3 relations chosen among Eqs.(10)÷(14)), the oxygen abundance $(O/H)_{T_e}$ in an H II region can then be determined.

3.2 An alternative version of the T_e method

Examination of Eq.(6) shows that the fluxes used to calculate R_3 and in the H_β line originate from different volumes of the nebula. The H_β flux comes from the whole H II region while the R_3 fluxes come from the volume where the oxygen is in the O^{++} stage. If Eq.(6) is applied to the O^{++} zone only, then it gives the total $\frac{O}{H}$ instead of the ionic $\frac{O^{++}}{H^+}$ oxygen abundance as in the traditional approach. In that case, Eq.(6) takes the form

$$12 + \log(O/H) = \log(I_{[OIII]\lambda4959+\lambda5007}/(w \times I_{H_\beta})) + 6.200 + \frac{1.251}{t_3} - 0.55\log t_3 - 0.014\,t_3, \quad (15)$$

where w is the fraction of the H_β flux in the O^{++} zone. With the adopted notations, Eq.(15) can be rewritten as

$$12 + \log(O/H) = \log(R_3/w) + 6.200 + \frac{1.251}{t_3} - 0.55\log t_3 - 0.014\,t_3. \quad (16)$$

Similarly, Eq.(7) can be rewritten as

$$12 + \log(O/H) = \log(I_{[OII]\lambda3727+\lambda3729}/[(1-w) \times I_{H_\beta}] + 5.961 + \frac{1.676}{t_2} - 0.40\log t_2 - 0.034\,t_2 + \log(1 + 1.35x_2). \quad (17)$$

or

$$12 + \log(O/H) = \log[R_2/(1-w)] + 5.961 + \frac{1.676}{t_2} - 0.40\log t_2 - 0.034\,t_2 + \log(1 + 1.35x_2). \quad (18)$$

There is no reason to expect the oxygen abundance in the O^{++} zone to differ from that in the O^+ zone within the same H II region. In other words, the oxygen abundance derived from Eq.(16) must be equal to the one derived from Eq.(18). Equating the right-hand sides of these two equations result in

$$\log(R_3/w) + 6.200 + \frac{1.251}{t_3} - 0.55\log t_3 - 0.014\,t_3 = \log[R_2/(1-w)] + 5.961 + \frac{1.676}{t_2} - 0.40\log t_2 - 0.034\,t_2 + \log(1 + 1.35x_2). \quad (19)$$

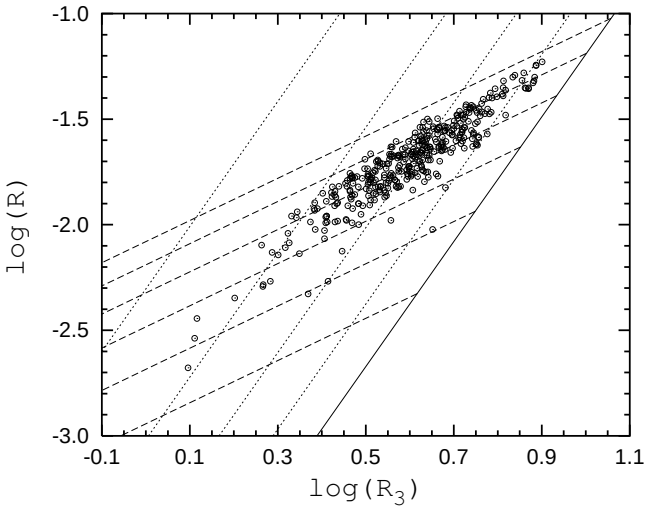

Figure 2. The R vs. R_3 diagram. The circles show individual H II region measurements from the standard sample. The relation corresponding to Eq.(20) for the value of the excitation parameter P = 1.0 is shown by the solid line. The dotted lines show from right to left the relations corresponding to that equation for P = 0.8, 0.6, 0.4 and 0.2. The dashed lines show from top to bottom the positions of H II regions with a given value of the electron temperature t_3 = 1.2, 1.1, 1.0, 0.9, 0.8 and 0.7, in units of 10^4 K.

Eq.(19) can be solved for t_2 if the values of t_3, n_e and w are known. The majority of extragalactic H II regions are in the low-density regime (Zaritsky et al. 1994; Bresolin et al. 2005). Therefore we adopt an electron density $n_e = 100$ cm^{-3} for all the H II regions in our sample. Thus, Eq.(19) allows to derive the electron temperature t_2 within the [O II] zone in a H II region if the electron temperature t_3 within the [O III] zone and the fraction w of H_β flux in the O^{++} zone are known.

3.3 Estimation of the parameter w

The fraction w of H_β flux in the O^{++} zone can be estimated in the following way. We have investigated recently the relationship between the observed auroral and nebular oxygen line fluxes in spectra of H II regions (Pilyugin 2005; Pilyugin et al. 2006). We have found a relation (called the ff relation) that is metallicity-dependent at low metallicities, but independent of metallicity above 12+logO/H $\sim$ 8.25, i.e. there is one-to-one correspondence between the auroral and nebular oxygen line fluxes in spectra of high-metallicity H II regions. Using a compilation of recent high-precision measurements of oxygen lines fluxes in high-metallicity H II regions, the following ff relation was derived (Pilyugin et al. 2006)

$$\begin{aligned} \log R &= -4.151 - 3.118 \log P + 2.958 \log R_3 \\ &- 0.680 (\log P)^2. \end{aligned} \quad (20)$$

Fig. 2 shows the relation corresponding to Eq.(20) in the R_3 – R diagram for various values of the excitation parameter P. The solid line, called hereafter as the basic line, corresponds to P = 1.0, while the dotted lines correspond, from right to left, to P = 0.8, 0.6, 0.4, 0.2. The dashed lines show the loci of H II regions for several values of the electron temperature t_3. From top to bottom, t_3 = 1.2, 1.1, 1.0, 0.9, 0.8, 0.7 in units of 10^4 K. The circles show individual measurements of H II regions from the present sample.

Let us consider a sequence of H II regions with the same value of t_3. The fraction of radiation of the H II region in the O^{++} zone increases along this sequence from low to high values of P, and reaches its maximum value, $w = 1$, at P = 1, i.e. at the intersection point of a dashed line with a given electron temperature with the basic solid line . Then, the fraction of radiation in the O^{++} zone can be estimated as

$$w = R_3^{\rm obs} / R_3^{\rm P=1}. \quad (21)$$

Such an estimate is not airtight since not only w can change along a sequence of H II regions with a fixed value of t_3, but other characteristics of H II regions, such as, for example, their oxygen abundance, can do so as well. Therefore, the value of t_2^* derived from Eq.(19) and Eq.(21) may carry some systematic error E_t. That error should be small for high-excitation H II regions (they are located close to the basic line) but increase with decreasing P. In the following, we discuss how to estimate that error and correct t_2^* for it.

4 THE t_2–t_3 RELATION

The top panel in Fig. 3 shows the value of t_2^* as derived from Eq.(19) and Eq.(21) for the objects in our standard subsample of high-metallicity H II regions. As noted above, t_2^* has a systematic error E_t that depends on the value of the excitation parameter P. To illustrate the point, we show in the bottom panel of Fig. 3 high quality data (those with $|D_{\rm ff}| < 0.01$) for H II regions with $0.9 > P > 0.8$ (filled circles) and for those with $0.5 > P > 0.4$ (open circles). Inspection of the bottom panel in Fig. 3 shows that indeed the $t_2^* - t_3$ relations are slightly different for H II regions with different values of P: at a given value of t_3, $t_2^* = t_2 + E_t$ is slightly smaller, on average, for low than for high excitation H II regions. The true $t_2 - t_3$ relation can be found by extrapolation of the $t_2^* - t_3$ relation to P = 1.

The bottom panel in Fig. 3 shows that the systematic error E_t is small. Therefore, we will approximate it by a linear expression, i.e. the true t_2 and the derived t_2^* values are related by

$$t_2 = t_2^* - E_t = t_2^* - c\,(1 - P). \quad (22)$$

Examination of Fig. 3 shows also that the $t_2 - t_3$ relation can be parametrized as

$$t_2 = a\,t_3 + b. \quad (23)$$

The coefficients a and b in Eq.(23) and the coefficient c in Eq.(22) can be found simultaneosly by fitting the data in the top panel of Fig. 3) by an expression of the type

$$t_2^* = a\,t_3 + b + c\,(1 - P). \quad (24)$$

Carrying out a standard least-squares fit to the data, we obtain the following values of the coefficients; $a = 0.716 \pm 0.012$, $b = 0.264 \pm 0.013$, $c = -0.042 \pm 0.007$. Then, the true $t_2 - t_3$ relation is

$$t_2 = 0.716(\pm 0.012)\,t_3 + 0.264(\pm 0.013). \quad (25)$$

The value of w given by Eq.(21) is the fraction of radiation in the O^{++} zone if the condition t_2=t_3 holds. This

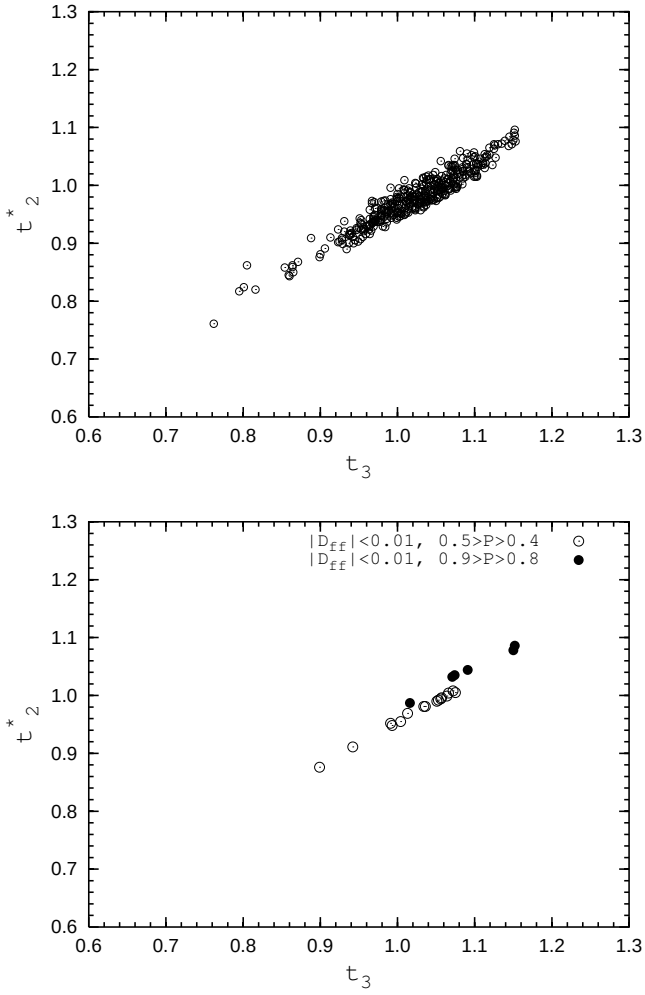

Figure 3. *Top panel.* The electron temperatures t_2^* versus t_3 for our standard sample of H II regions. *Bottom panel.* The same as in the top panel, except that only high-quality data with $|D_{ff}| < 0.01$ are included. Filled circles show H II regions with $0.9 > P > 0.8$, and open circles those with $0.5 > P > 0.4$.

is not however the case. Since the H_β emission coefficient, $E^0_{4,2}$, is dependent on the electron temperature (Aller 1984)

$$E^0_{4,2} = 1.387\, t^{-0.983}\, 10^{-0.0424/t}, \tag{26}$$

then the contribution w_c of the [OIII] zone to the total flux of the nebula in the H_β line is given by the following expression

$$w_c = \frac{E^0_{4,2}(t_3)\; w}{E^0_{4,2}(t_3)\; w + E^0_{4,2}(t_2)\; (1-w)}. \tag{27}$$

We have recomputed the values of t_2^* using w_c instead of w. We found the differences between the t_2^* values derived with w and w_c to be less than 0.01. Therefore, we will neglect this small correction, and will use the value of w given by Eq.(21).

We now check whether the linear forms of the analytical expressions adopted for the t_2 – t_3 and t_2^* – t_2 relations are justified. The top panel of Fig. 4 shows the difference Δt_2^* between the value of t_2^* derived from Eq.(19) and Eq.(21) and the one derived from Eq.(24) as a function of the excitation parameter P. The points are individual measurements of H II regions from the standard subsample, and the line is

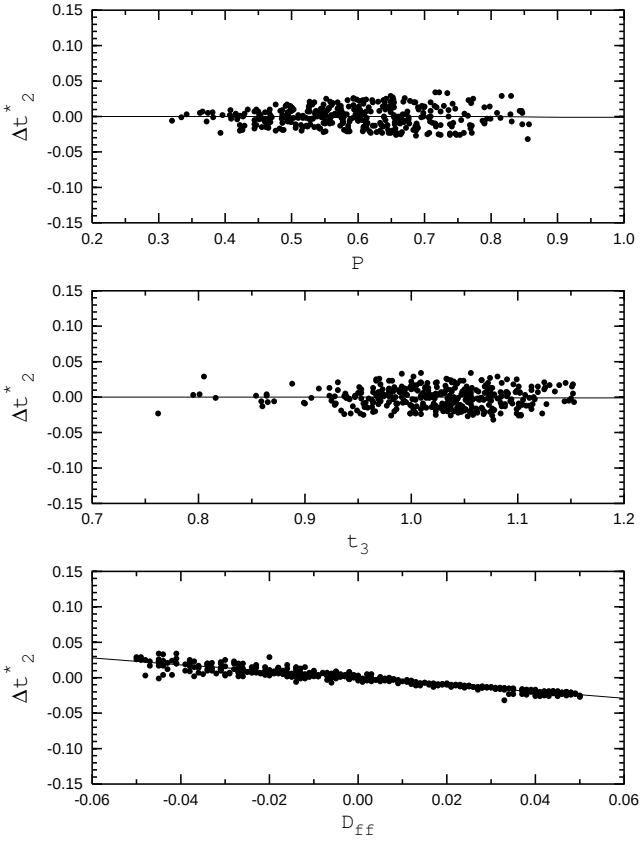

Figure 4. The difference Δt_2^*, defined in section 4, as a function of excitation parameter (*top panel*), electron temperature t_3 (*middle panel*), and discrepancy index D_{ff} (*bottom panel*) for our standard sample of H II regions.

the linear best fit to those data obtained through the least-squares method. The middle panel in Fig. 4 shows the same difference Δt_2^* as a function of the electron temperature t_3. Examination of the top and middle panels of Fig. 4 shows that Δt_2^* does not coorelate either with P or t_3, justifying our adoption of linear forms for the t_2 – t_3 and t_2^* – t_2 relations.

The bottom panel in Fig. 4 shows Δt_2^* as a function of the discrepancy index D_{ff}. There is an anticorrelation of the two quantities. Since the discrepancy index appears to be an indicator of the error in the auroral line R measurements, this suggests that the t_2 – t_3 correlation is rather tight, and that any scatter in this correlation is caused mainly by uncertainties in the measurements.

The low uncertainty in the values of the coefficients in Eq.(25) may be a consequence of the large number of points (372) used. The following consideration can tell us something about the true accuracy of the derived t_2 – t_3 relation. We have extracted from our standard sample a subsample of 86 high-quality measurements of H II regions with $|D_{ff}| < 0.01$. The derived t_2^* – t_3 diagram for this subsample is shown in the top panel of Fig. 5. A fit to those data gives

$$t_2^* = 0.729\,(\pm 0.006)\, t_3 + 0.257\,(\pm 0.007) \\ -0.058\,(\pm 0.003)\,(1-P) \tag{28}$$

The corresponding t_2 – t_3 relation is then

$$t_2 = 0.729\,(\pm 0.006)\, t_3 + 0.257\,(\pm 0.007). \tag{29}$$

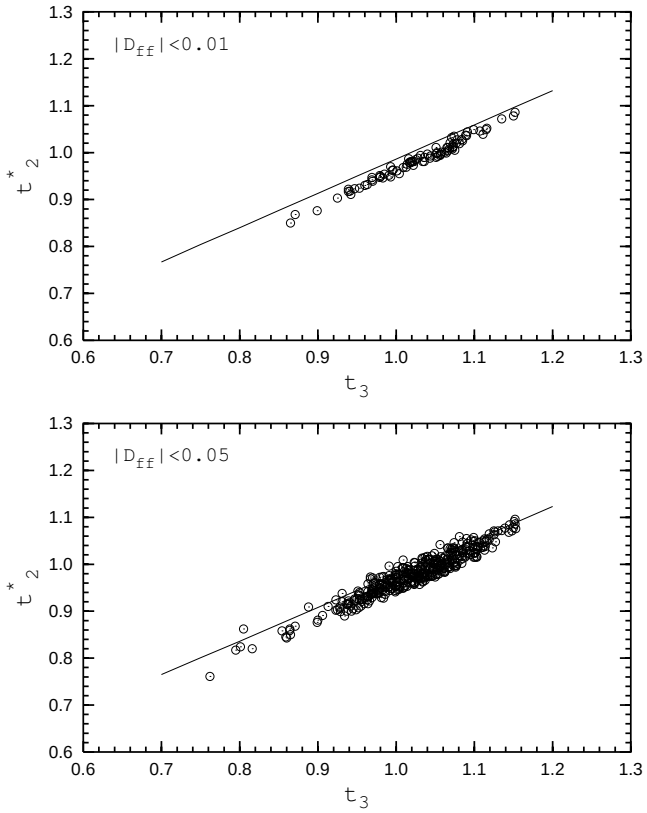

Figure 5. Open circles show the t_2^* – t_3 diagram for the subsample of H II regions with $|D_{ff}| < 0.01$ (*top panel*), and for the standard sample (*bottom panel*).

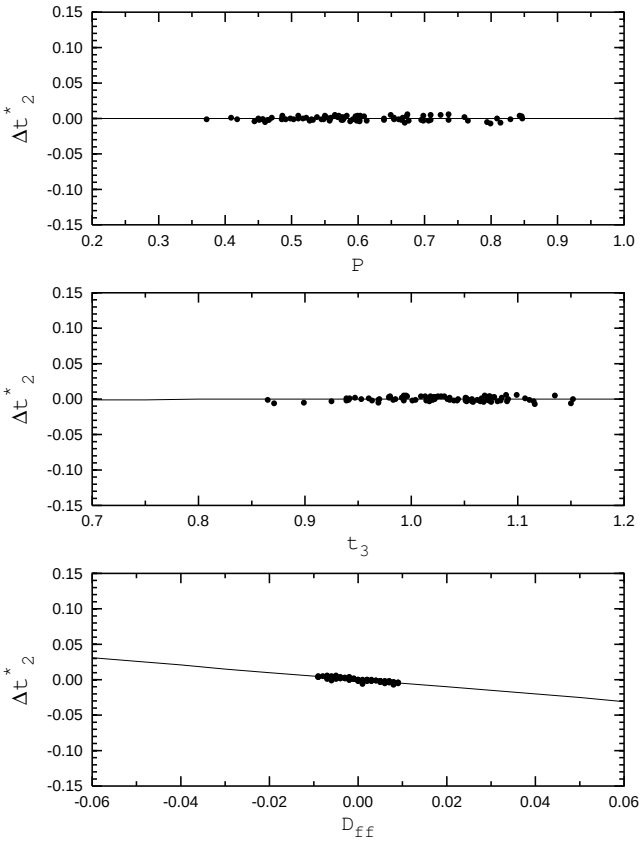

Figure 6. The difference Δt_2^*, defined in section 4, as a function of excitation parameter P (*top panel*), electron temperature t_3 (*middle panel*), and discrepancy index D_{ff} (*bottom panel*) for the subsample of H II regions with $|D_{ff}| < 0.01$.

This relation is shown by the solid line in the top panel of Fig. 5. For comparison, the bottom panel of Fig. 5 shows the t_2^* – t_3 diagram and the t_2 – t_3 relation for the whole standard sample.

Fig. 6 shows the differences Δt_2^* between the values of t_2^* derived from Eq.(19) and Eq.(21) and the one derived from Eq.(28) as a function of P (top panel), t_3 (middle panel) and D_{ff} (bottom panel). The points are individual H II regions with $0.01 > D_{ff} > -0.01$, the lines are linear least-square fits to those data. Comparison of Fig. 4 and Fig. 6 shows clearly that the scatter in t_2 at a fixed value of t_3 decreases in the subsample of H II regions with more precise measurements. This confirms our conclusion that the t_2 – t_3 correlation is rather tight, and that the scatter in it is caused mainly by measurement uncertainties.

Examination of Eq.(25) and Eq.(29) shows that the t_2 – t_3 relations derived from the two different samples of H II regions are very similar and agree within the formal uncertainties. Thus the derived t_2 – t_3 relation is rather robust. In the following, we will adopt as the t_2 – t_3 relation

$$t_2 = 0.72\, t_3 + 0.26 \qquad (30)$$

We note that it has been generally accepted that there is a one-to-one correspondence between t_2 and t_3, i.e. that the t_2 – t_3 relation does not depend on an additional parameter. If there is a dependence of the t_2 – t_3 relation on the excitation parameter (from general considerations, this cannot be excluded), that dependence cannot be revealed by our approach and can influence the derived relation.

In summary, there is a tight correlation between the electron temperature t_3 within the [O III] zone and the electron temperature t_2 within the [O II] zone in high-metallicity H II regions. This correlation can be well approximated by a linear expression and its form is rather robust.

5 DISCUSSION

We now compare the t_2 – t_3 relation obtained here with those obtained by other authors. Fig. 7 shows our t_2 – t_3 relation together with those from Campbell et al. (1986); Pagel et al. (1992); Izotov et al. (1997); Deharveng et al. (2000); Oey & Shields (2000). Since our t_2 – t_3 relation is derived for cool high-metallicity H II regions then the high-temperature low-metallicity part of relation is not considered here. Fig. 7 shows that our t_2 – t_3 relation is most similar to the one by Campbell et al. (1986).

We consider next how the obtained t_2 – t_3 relation may affect the derived oxygen abundances in H II regions. Since the t_2 – t_3 relation of Campbell et al. (1986) has found wide acceptance and use in abundance determinations in H II regions, we will compare oxygen abundances derived with the Campbell et al. (1986) relation and ours. For this purpose, we use the data for H II regions in the spiral galaxy NGC 4254 obtained by McCall et al. (1985); Shields et al. (1991); Henry et al. (1994). Since the auroral [O III]λ4363

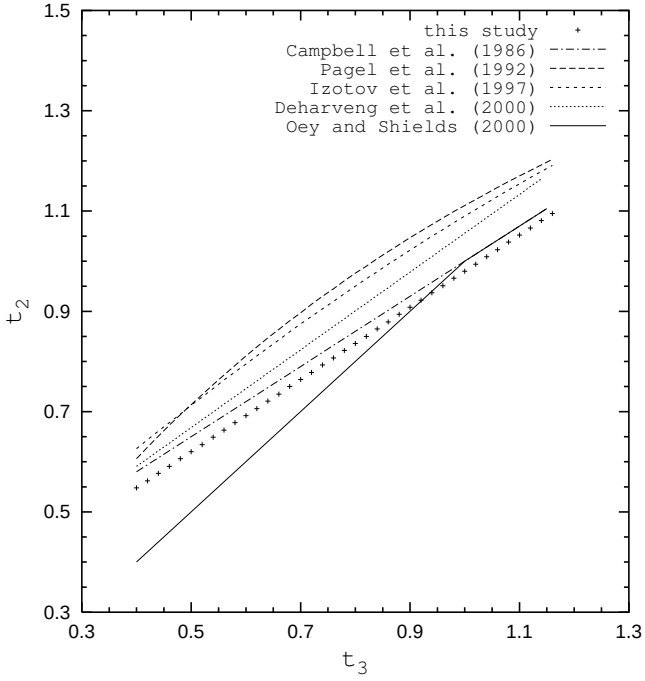

Figure 7. Comparison of the t_2 – t_3 relation derived here with those derived by other investigators.

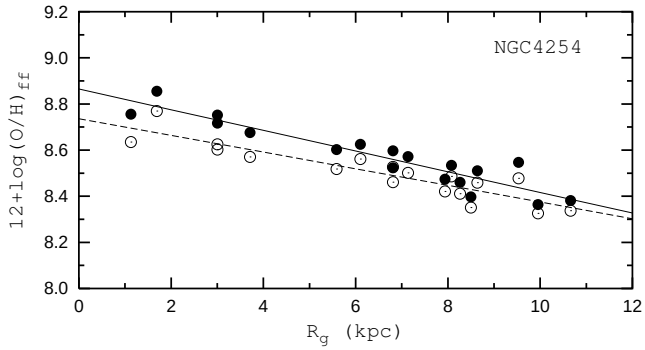

Figure 8. The radial distribution of oxygen abundances across the disk of the spiral galaxy NGC 4254. The filled circles show $(O/H)_{ff}$ abundances based on the t_2 – t_3 relation derived in the present study, and the solid line is the linear least-squares best fit to those data. The open circles show $(O/H)_{ff}$ abundances based on the t_2 – t_3 relation of Campbell et al. (1986), and the dashed line is the linear least-squares best fit to those data.

line was not detected in those H II regions, $O/H)_{ff}$ abundances based on the line fluxes R^{cal} have been determined from the ff relation, Eq.(20), for every H II region, following Pilyugin et al. (2006). The $(O/H)_{ff}$ abundances in the H II regions of NGC 4254 determined using the t_2 – t_3 relation of Campbell et al. (1986) are shown as a function of galactocentric distance in Fig. 8 by open circles. The dashed line is the linear least-squares best fit to those data:

$$12 + \log(O/H) = 8.74\,(\pm0.03) - 0.036\,(\pm0.004) \times R_g. \quad (31)$$

We have adopted a distance of 16.14 Mpc for NGC 4254 (Pilyugin et al. 2004). The filled circles are $(O/H)_{ff}$ abundances determined with our t_2 – t_3 relation. The solid line is the linear least-squares best fit to those data:

$$12 + \log(O/H) = 8.86\,(\pm0.03) - 0.045\,(\pm0.004) \times R_g. \quad (32)$$

Fig. 8 shows that the abundances derived with our t_2 – t_3 relation are slightly higher (up to $\sim$ 0.1 dex) than those derived with the relation by Campbell et al. (1986). Comparison of Eq.(31) and Eq.(32) leads to the same conclusion.

6 CONCLUSIONS

We suggest a new way to establish the relation between the electron temperature t_3 within the [O III] zone and the electron temperature t_2 within the [O II] zone in high-metallicity (12+log(O/H) > 8.25) H II regions. The basic idea is the following. If we apply the equation used to calculate the ionic abundance O^{++}/H^+ not to the entire H II region but only to the O^{++} zone, then this would yield, not the ionic O^{++}/H^+ abundance but the total O/H oxygen abundance instead. We require that the equation for O^{++}/H^+ applied to the O^{++} zone and the one for O^+/H^+ applied to the O^+ zone result in exactly the same value of the oxygen abundance. This condition allows us to derive a relation between t_2 and t_3. We have applied this method to a sample of 372 H II regions selected to have high-quality measurements by using the ff relation (Pilyugin et al. 2006). We find that the correlation between t_2 and t_3 is tight and can be approximated by a linear expression. The so derived $t_2 - t_3$ relation is independent of photoionization models of H II regions.

The derived relation can be used to determine t_2 and accurate abundances in high-metallicity H II regions with a measured t_3 temperature. It can be also used in conjunction with the ff relation of Pilyugin et al. (2006) for the determination of the t_3 and t_2 temperatures and oxygen abundances in high-metallicity H II regions where the [OIII]λ4363 auroral line is not detected.

Our t_2 – t_3 relation is close to the widely used relation of Campbell et al. (1986). However, the abundances derived with our t_2 – t_3 relation are slightly higher (up to $\sim$ 0.1 dex) than those derived with the Campbell et al. (1986) relation.

Acknowledgments

We thank Yuri Izotov and Natalia Guseva for providing us with their measurements of the line intensities in spectra of H II regions extracted from the Data Release 3 of the Sloan Digital Sky Survey (SDSS), the majority of which are not published. We are grateful to Bernard Pagel for a numerous constructive comments over all the period of the performance of this study. We thank the anonymous referee for helpful comments. This research was made possible in part by Award No. UP1-2551-KV-03 of the US Civilian Research & Development Foundation for the Independent States of the Former Soviet Union (CRDF). T.X.T. has been partially supported by NSF grant AST-02-05785. T.X.T. thanks the hospitality of the Institut d'Astrophysique in Paris and of the Service d'Astrophysique at Saclay during his sabbatical leave. He is grateful for a Sesquicentennial Fellowship from the University of Virginia. All the authors acknowledge the work of the SDSS team. Funding for the SDSS has been provided by the Alfred P. Sloan Foundation, the Participating Institutions, the National Aeronautics and Space Administration, the National Science Foun-

dation, the U.S. Department of Energy, the Japanese Monbukagakusho, and the Max Planck Society. The SDSS Web site is http://www.sdss.org/. The SDSS is managed by the Astrophysical Research Consortium (ARC) for the Participating Institutions. The Participating Institutions are The University of Chicago, Fermilab, the Institute for Advanced Study, the Japan Participation Group, The Johns Hopkins University, the Korean Scientist Group, Los Alamos National Laboratory, the Max-Planck-Institute for Astronomy (MPIA), the Max-Planck-Institute for Astrophysics (MPA), New Mexico State University, University of Pittsburgh, University of Portsmouth, Princeton University, the United States Naval Observatory, and the University of Washington.

REFERENCES

Aller L.H., 1984, Physics of thermal gaseous nebulae, D. Reidel Publishing Company, Dordrecht.
Bresolin F., Schaerer D., González Delgado R.M., Stasińska G., 2005, A&A, 441, 981
Campbell A., Terlevich R., Melnick J., 1986, MNRAS, 223, 811
Deharveng L., Peña M., Caplan J., Costero R., 2000, MNRAS, 311, 329
Garnett D.R., 1992, AJ, 103, 1330
Henry R.B.C., Pagel B.E.J., Chincarini G.L., 1994, MNRAS, 266, 421
Izotov Y.I., Stasińska G., Guseva N.G., Thuan T.X., 2004, A&A, 415, 87
Izotov Y.I., Stasińska G., Meynet G., Guseva N.G., Thuan T.X., 2006, A&A, 448, 955
Izotov Y.I., Thuan T.X., Lipovetsky V.A., 1997, ApJS, 108, 1
Kennicutt R.C., Bresolin F., Garnett D.R., 2003, ApJ, 591, 801
McCall M.L., Rybski P.M., Shields G.A., 1985, ApJS, 57, 1
Oey M.S., Shields J.C., 2000, ApJ, 539, 687
Pagel B.E.J., Simonson E.A., Terlevich R.J., Edmunds M.G., 1992, MNRAS, 255, 325
Pilyugin L.S., 2005, A&A, 436, 1L
Pilyugin L.S., Thuan T.X., 2005, ApJ, 631, 231
Pilyugin L.S., Thuan T.X., Vílchez J.M., 2006, MNRAS, 367, 1139
Pilyugin L.S., Vílchez J.M., Contini T., 2004, A&A, 425, 849
Rubin R.H., 1986, ApJ, 309, 334
Shields G.A., Skillman E.D., Kennicutt R.C., 1991, ApJ, 371, 82
Stasińska G., 1982, A&AS, 48, 299
Stasińska G., 1990, A&AS, 83, 501
Stasińska G., Schaerer D., 1997, A&A, 322, 615
Tsamis Y.G., Barlow M.J., Liu X.-W., Danziger I.J., Storey P.J., 2003, MNRAS, 338, 687
Zaritsky D., Kennicutt R.C., Huchra J.P., 1994, ApJ, 420, 87